Bonding and Electronic Properties of Cs_3Te_{22}

F. Boucher* and R. Rousseau

Max-Planck Institut für Festkörperforschung, Heisenberg Strasse 1, D-70569 Stuttgart, Germany

Received November 19, 1997

The compound Cs_3Te_{22} is well-known for its interesting structural features. It contains both a unique 2,3-connected defect square Te sheet and Te_8 rings. For a better understanding of the structure and bonding, the band structure of Cs_3Te_{22} is examined by means of the ab initio tight-binding linear muffin-tin orbital (TB-LMTO) method, which is based upon density functional theory (DFT). The calculations are complemented by an analysis of the electronic density topology with the electron localization function (ELF) and a traditional orbital analysis using the projected density of states (DOS) and the crystal orbital Hamiltonian population (COHP). Our study indicates that the short Te−Te contacts between Te_8 rings and the defect Te_6^{3-} sheet in this compound have a direct influence upon the properties of this material. The presence of this interaction perturbs the electronic density relative to that which one obtains from analysis of the isolated defect sheet and leads to favorable conditions for an insulator state.

Introduction

The study of low-dimensional inorganic conducting solids has been a major field of research for the last 20 years. A central role in this research has been played by the family of compounds formed by metal chalcogenides.[1] These materials exhibit many interesting phenomena such as spin density waves (SDW), charge density waves (CDW), and superconductivity.

Recently, a new family of materials, the alkali metal tellurides, has generated a significant amount of interest due to their potential as new low-dimensional metals.[2] This family of compounds is unique in that the alkali metal atom interacts with the tellurium atoms to form a template by which novel structural motifs such as defect square sheets and rings may be formed. These species exhibit a rich diversity of structural fragments[3] including $(Te_n)^{m-}$ rings,[4] infinite Te chains,[5] and layers.[6] It has been noted that many of these fragments may be understood in terms of simple model concepts.[7] However, of most interest to the materials science community is the presence of defect square sheets. These sheets have been known in chalcogenide chemistry to be intimately linked with CDW states and metallic conductivity. For example, the compound $K_{0.33}Ba_{0.67}AgTe_2$ has such a defect square lattice and is found to exist in a CDW state at room temperature, which destroys metallic conductivity.[8]

Recently, the material Cs_3Te_{22} was reported,[9] which contains both a unique 2,3-connected defect square sheet and the long sought after Te_8 ring. This compound is of a considerable interest to the community of theoretical chemists due to these unique structural features. To date, there have been three theoretical studies on this compound. The first, by Lee and Foran,[10] discusses the defect square lattice of this compound in terms of a model based on the Fermi surface of nondefective lattices. Liu, Goldberg, and Hoffman[11] have performed an extensive study on this same sheet by comparison with similar structural units in order to understand structure/bonding relationships. The latter authors conclude from their study that this compound may "be conducting or magnetic" in terms of its properties. Canadell and co-workers[2,12] have performed a similar study where they conclude that the system could be metallic and that the Fermi surface of this compound presents an ideal situation for nesting and may lead to either a CDW or SDW state. These studies have been performed with the tight-binding extended Hückel method (eH) (or a variation thereof[10]) and predominantly focus on the analysis of the results for the isolated defect square sheet with an appropriate 3− charge as dictated by the Zintl−Klemm concept. Normally, these types of approximations have been shown to be excellent for low-dimensional solids.[13] However, if this material is indeed an insulator with a half-filled band, one may perhaps wish to use a more sophisticated electronic structure method to obtain a deeper understanding of the localized states where explicit modeling of electron−electron interactions is of paramount importance. Furthermore, within this compound there are several short Te−Te distances of about 3.4 Å (which is

* Corresponding author. Permanent address: Institut des Matériaux de Nantes, UMR C 6502 CNRS−Université de Nantes, BP 32229, 44322 Nantes Cedex 3, France. E-mail: boucher@cnrs-imn.fr.

(1) Meerschaut, A.; Rouxel, J. In *Crystal Chemistry and Properties of Materials of Quasi-One-Dimensional Structures*; Rouxel, J., Ed.; Reidel: Dordrecht, The Netherlands, 1986.
(2) Sheldrick, W. S.; Wachhold, M.; Jobic, S.; Brec R.; Canadell, E. *Adv. Mater.* **1997**, *8*, 669.
(3) Böcher, P. *Angew Chem., Int. Ed. Engl.* **1988**, *27*, 759.
(4) See for example the following structures. K_2Te_3: Eisenmann, B.; Shcäffer, H. *Angew Chem., Int. Ed. Engl.* **1978**, *17*, 684. $CsTe_4$: Böttcher, P.; Kretschmann, U. *Z. Anorg. Allg. Chem.* **1985**, *523*, 145. $NaTe_3$: Böttcher, P.; Keller, R. *Z. Anorg. Allg. Chem.* **1986**, *542*, 144. K_2Te_2: Schreiner, B.; Dehnicke, K.; Maczek, K.; Fenske, D. *Z. Anorg. Allg. Chem.* **1993**, *619*, 1414.
(5) Böttcher, P.; Kretschmann, U. *J. Less-Common Met.* **1983**, *95*, 81.
(6) Scheldrick, W. S.; Schaff, B. *Z. Naturforsch., B* **1994**, *49*, 993.
(7) Kanatzidis, M. G. *Angew. Chem., Int. Ed. Engl.* **1995**, *34*, 2109.
(8) Zhang, X.; Li, J.; Foran, B.; Lee, S.; Gou, H.-Y.; Hogan, T.; Kannerworth, C. R.; Kanatzidis, M. G. *J. Am. Chem. Soc.* **1995**, *117*, 10513.
(9) Sheldrick, W. S.; Wachhold, M. *Angew. Chem., Int. Ed. Engl.* **1995**, *34*, 450.
(10) Lee, S.; Foran, B. *J. Am. Chem. Soc.* **1996**, *118*, 9139.
(11) Liu, Q.; Goldberg N.; Hoffmann, R. *Chem−Eur. J.* **1996**, *2*, 390.
(12) Jobic, S.; Sheldrick, W. S.; Canadell, E.; Brec., R. *Bull. Soc. Chim. Fr.* **1996**, *133*, 221.
(13) Canadell, E.; Whangbo, M.-H. *Chem. Rev.* **1991**, *91*, 965.

S0020-1669(97)01460-2 CCC: $15.00
Published on Web 04/28/1998

significantly shorter than the van der Waals distance of 3.8 Å for the Te−Te interaction) between the Te_8 rings and this defect square sheet. One may suppose that these close contacts between apparently isolated structural components may alter the electronic structure of either the rings or the sheet and, therefore, the conductivity properties of this material. Thus, it may not be altogether clear how appropriate such approximate structural models are for providing an accurate picture of the structure and bonding for this particular compound.

Toward this end, we have undertaken a new electronic band structure study of the compound Cs_3Te_{22} by using the tight-binding linear muffin-tin orbital method in the atomic spheres approximation (TB-LMTO-ASA or LMTO for short).[14] This method, which is based upon density functional theory (DFT),[15] implicitly includes an accurate model of the electronic energy and has been shown to give reliable results for several low-dimensional solids.[16] By inclusion of a more accurate description of charge transfer, one can examine the whole unit cell including the Te_8 rings, the square sheets, and the Cs atoms without resorting to any approximations of the structure. Furthermore, the LMTO method supplies reliable electronic densities that may be analyzed in terms of either orbitals or electron localization functions. Therefore, we have chosen to investigate this structure using the electron localization function (ELF) of Becke and Edgecombe,[17a] which has been widely used as an interpretative tool for both molecules and solids.[17b−d] By combining this method with traditional orbital analysis, we provide a picture of the relationship among crystal structure topology, bonding, and the electronic properties of Cs_3Te_{22}.

Computational Aspects

The self-consistent ab initio band structure calculations of Cs_3Te_{22} were performed with the TB-LMTO-ASA method.[14] Exchange and correlation were treated in the local density approximation using the von Barth−Hedin local exchange correlation potential.[18a] All relativistic effects except spin−orbit coupling were taken into account using the scalar relativistic approximation.[18b] Under the ASA, one assumes that space can be filled with small overlapping Wigner−Seitz (WS) atomic spheres. The potential symmetry is considered spherical within the spheres; an appropriate correction (the combined correction)[16a] is used to take into account the overlap between spheres. The radii of WS spheres were determined by the condition that the overlapping potential be the best possible approximation to the full potential. The values of the sphere radii were found in accordance with the procedure outlined in ref 16a. Within the LMTO formalism interatomic spaces are filled with interstitial spheres. The optimal positions and radii of these additional "empty spheres" (ES) were determined by a procedure also described in ref 16a. As a result of the overlapping spheres and the subsequent correction, the kinetic energy is in error, the magnitude of which is proportional to the fourth power of the relative sphere overlap. Thus, the overlap should be minimized to values of about 15%.[16a] Since symmetrically inequivalent atoms have different coordination environments, and hence overlap in different ways with adjacent spheres, they will not have exactly the same sphere radii in order to best match the full potential. In total, six non-symmetry-related ES with $0.91\ \text{Å} \leq r_{ES} \leq 1.21\ \text{Å}$ were introduced for the calculation. In this way, the maximum relative overlap between two adjacent atomic spheres was minimized to an appropriate value (<15.5%).

The full LMTO basis set consisted of the 6s, 6p, 5d, and 4f functions for the Cs spheres, the 5s, 5p, 5d, and 4f functions for the Te spheres, and the s, p, and d functions for the empty spheres (ES). The eigenvalue problem was solved using the following minimal basis set obtained from the Löwdin downfolding technique: Cs (6s), Te (5s and 5p) and ES (1s) LMTO's. We denote this basis set as the β representation. The **k**-space integration was performed using the tetrahedron method.[18c] Charge self-consistency and the average properties were obtained from 78 irreducible **k**-points. The atomic parameters used for the calculation (sphere radii and positions of the ES) are given in ref 19.

A measure of the magnitude of bonding was obtained by computing the COHP (crystal orbital Hamiltonian population)[20a] which is the Hamiltonian population weighted density of states. The COHP function normally gives results similar to those of the well-known COOP. However, this function is much less basis set dependent, and therefore preferential for our LMTO calculations. As recommended,[20b] a reduced basis set (in which all the empty sphere LMTO's have also been downfolded) was used for the COHP calculation. More details about COHP calculations are given elsewhere.[20c]

For the sake of computational simplicity, we have chosen the primitive cell that contains half of the atoms of the body-centered cell.[21] This provides us with the new unit cell basis of $\mathbf{t_1} = {}^1/_2(-a, b, c)$, $\mathbf{t_2} = {}^1/_2(a, -b, c)$ and $\mathbf{t_3} = {}^1/_2(a, b, -c)$. We thus use the Brillouin zone (BZ) associated with this lattice (p 105 of ref 21) both for our **k**-space calculations and for the presentation of the band structure.

Results and Discussion

The Structure of Cs_3Te_{22}. We first present a brief description of the crystal structure of Cs_3Te_{22}. We illustrate this structure in Figure 1. In this figure, and throughout this work, we shall use the numbering scheme of the atoms according to ref 9. The compound crystallizes in the space group $I4/m$ with lattice vectors $a = b = 9.586$ Å and $c = 20.537$ Å. The unit cell of the compound contains two 2D slabs of formula unit $CsTe_6$ and four $CsTe_8$ layers. The stacking of these layers along the crystallographic c direction is shown in Figure 1a. Each layer consists of an isolated Cs atom and a Te_8 ring. The structure of this ring is analogous to that of both neutral S_8 and Se_8 rings. Furthermore, the average Te−Te bond length of 2.80 Å compares well with the value of 2.83 Å in elemental Te, which exists as helical chains of Te atoms. These facts strongly indicate that this ring is a neutral species.

The $CsTe_6$ slab itself is quite interesting. There are two distinct types of atoms that have strikingly different coordination environments. We illustrate the slab in Figure 1b. Te(4) is linearly coordinated with two bonds of 3.077 Å to Te(3) atoms. This is in contrast to the Te(3) site, which together with the

(14) Andersen, O. K. *Phys. Rev. B* **1975**, *12*, 3060. Andersen, O. K.; Jepsen, O. *Phys. Rev. Lett.* **1984**, *53*, 2571. Andersen, O. K.; Jepsen, O.; Glötzel, D. In *Highlights of condensed-matter theory*; Bassani, F., Fumi, F., Eds.; North Holland: New York, 1985. Lambrecht, W. R. L.; Andersen, O. K. *Phys. Rev. B* **1986**, *34*, 2439.

(15) (a) Parr, R.; Yang W. In *The Denisty Functional Theory of Atoms and Molecules*; Oxford: New York, 1989. (b) Jones, R. O.; Gunnarson, O. *Rev. Mod. Phys.* **1989**, *61*, 689.

(16) (a) Jepsen, O.; Andersen, O. K. *Z. Phys. B* **1995**, *97*, 35. (b) Boucher, F.; Zhukov, Z.; Evain, M. *Inorg. Chem.* **1996**, *35*, 7649. Nesper, R.; Wengert, S. *Chem−Eur. J.* **1997**, *3*, 985.

(17) (a) Becke, A. D.; Edgecombe, N. E. *J. Chem. Phys.* **1990**, *92*, 5397. For interpretation of the results of this function see: (b) Silvi, B.; Savin, A. *Nature* **1994**, *371*, 683. (c) Savin, A.; Becke, A. D.; Flad, J.; Nesper, R.; Preuss, H.; von Schnering, H. G. *Angew. Chem., Int. Ed. Engl.* **1991**, *30*, 409. (d) Savin, A.; Jepssen, O.; Flad, J.; Andersen, O. K.; Preuss, H.; von Schnering, H. G. *Angew. Chem., Int. Ed. Engl.* **1992**, *31*, 187.

(18) (a) von Barth, U.; Hedin, L. *J. Phys. C* **1972**, *5*, 1629. (b) Koelling, D. D.; Harmon, B. N. *J. Phys. C* **1977**, *10*, 3107. (c) Blöchl, P. E.; Jepsen, O.; Andersen, O. K. *Phys. Rev. B* **1994**, *49*, 16223.

(19) Sphere radii: Cs(1), 2.80 Å; Cs(2), 2.80 Å; Te(1), 1.61 Å; Te(2), 1.61 Å; Te(3), 1.73 Å; Te(4), 1.82 Å. Empty sphere radii and positions: E(1), 1.21 Å || (${}^1/_2$, 0, 0.865); E(2), 1.20 Å || (${}^1/_2$, 0, ${}^3/_4$); E(3), 1.19 Å || (0.810, 0.387, 0.075); E(4), 1.04 Å || (0.751, 0.871, 0.273); E(5), 1.02 Å || (0.364, 0.957, 0.807); E(6), 1.00 Å || (0.310, 0.127, 0.096); E(7), 0.949 Å || (0.114, 0.049, 0.324); E(6), 0.908 Å // (0.344, 0.806, 0).

(20) (a) Dronskowski, R.; Blöchl, P. E. *J. Phys. Chem.* **1993**, *97*, 8617. (b) Jepsen, O.; Andersen, O. K. Personal communication. (c) Boucher, F.; Jepsen, O.; Andersen, O. K. Manuscript in preparation.

(21) Bradkey, C. J.; Cracknell, A. P. *The Mathematical Theory of Symmetry in Solids*; Clarendon Press: Oxford, U.K., 1972.

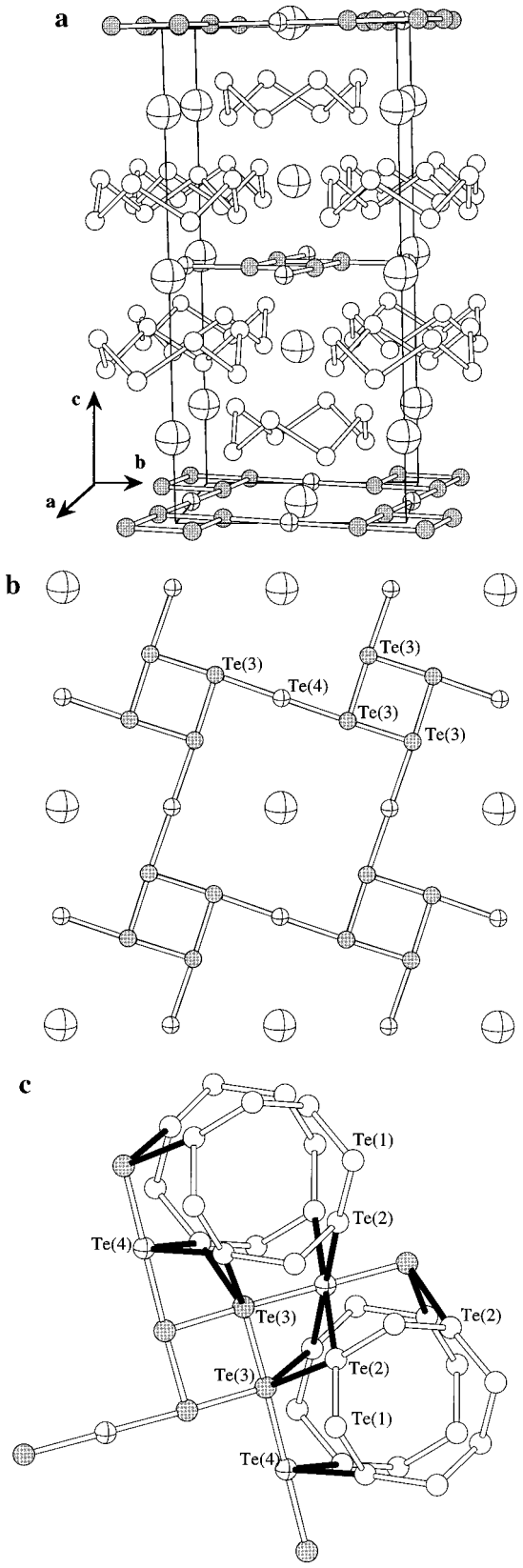

Figure 1. (a) Crystal structure of Cs_3Te_{22}. The Cs atoms have been represented with large crossed spheres, and the Te atoms with smaller spheres: open spheres, Te(1) and Te(2); shaded spheres, Te(3); crossed spheres, Te(4). (b) Projection along [001] of the $CsTe_6$ layer. (c) View of the Te−Te contacts between theTe_8 rings and the Te_6 layer.

bond to Te(4), has two more bonds to Te(3) atoms of 3.003 Å, forming a T structure. The Te(3) atoms form a square $Te(3)_4$ unit. These individual square units are linked via Te(4) atoms

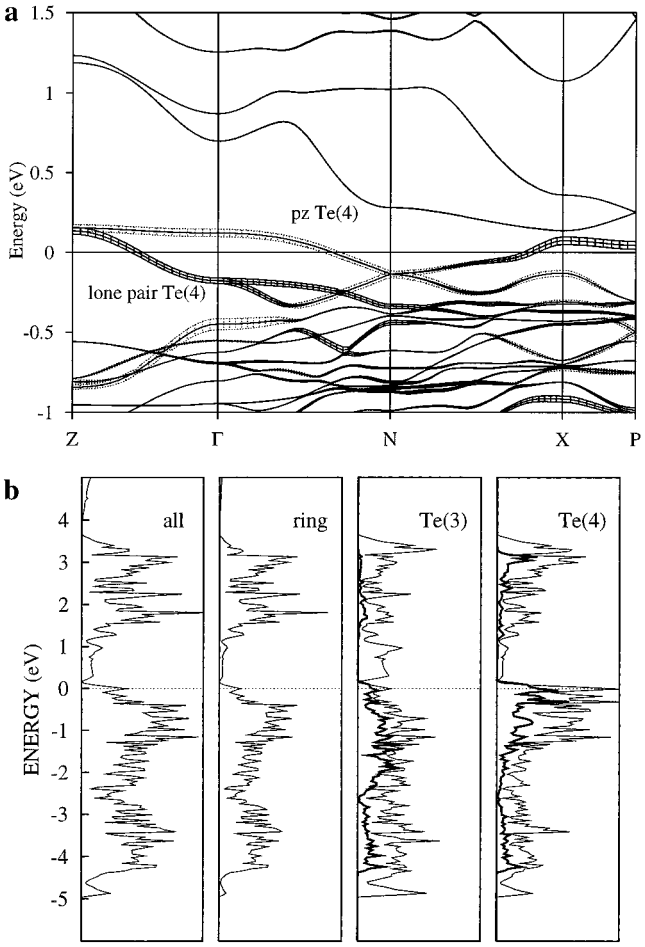

Figure 2. (a) Band structure of Cs_3Te_{22} (see the text for details about the **k** points used for the calculation). (b) Total density of states and Te_8 rings, Te(3), and Te(4) projected DOS for Cs_3Te_{22}. The out-of-plane p orbitals for Te(3) and Te(4) contributions are presented with wider lines. For convenience, a scale inversely proportional to the number of atoms is used for the projected DOS.

to form a defect 2D 2,3-connected network that lies parallel to the crystallographic *ab* plane. The above assignment of the Te_8 ring as a neutral species, combined with the Zintl−Klemm concept and an oxidation state assignment of +1 for the Cs atoms, ascribes a charge of 3− to the sheet. This odd number of electrons assigned to the 2D slab suggests that this compound may indeed be metallic or magnetic, but there have not been any physical measurements reported on this material. Therefore, it is not clear which of these possibilities is most likely.

Of the two symmetry-inequivalent Te atoms within the ring, the Te(2) atom is closest to the 2,3-connected sheet. This is illustrated in Figure 1c. The close contacts between Te(2) and the Te(3) and Te(4) atoms of the slab are 3.41 and 3.44 Å, respectively. These contacts are longer than the individual Te−Te bonds within the rings and the slab but are still shorter then the van der Waals distance by about 0.4 Å. The closest contacts between independent rings in the crystallographic *c* direction are on the order of magnitude of the 3.8 Å van der Waals distance between two Te atoms. Thus, the rings can be considered reasonably isolated from each other but perhaps not from the slab.

Structure and Bonding Relationships. To begin our development of structure and bonding relationships for Cs_3Te_{22}, we present the calculated band structure for the states near the Fermi level (E_F). These are shown in Figure 2a. For the sake of presentation, we set $E_F = 0$ eV in this figure and throughout

this work. For the band structure we display the dispersions along the directions Z−Γ, Γ−N, N−X, and X−P where Γ = (0, 0, 0), Z = ($\mathbf{g}_1$/2, $\mathbf{g}_2$/2, −$\mathbf{g}_3$/2), N = (0, $\mathbf{g}_2$/2, 0), X = (0, 0, $\mathbf{g}_3$/2), and P = ($\mathbf{g}_1$/4, $\mathbf{g}_2$/4, $\mathbf{g}_3$/4) with $\mathbf{g}_1$, $\mathbf{g}_2$, and $\mathbf{g}_3$ being the reciprocal vectors of the primitive cell ($\mathbf{t}_1$, $\mathbf{t}_2$, $\mathbf{t}_3$) as defined above.[21] The LMTO band structure of this compound reveals two bands that cross the Fermi level. The upper band at Γ, which has a total width of 0.3 eV, crosses E_F along the Γ−N direction. Inspection of the charge density reveals that this band is associated with Te 5p orbitals that are oriented perpendicular to the Te_6^{3-} slab. The second band, which is doubly degenerate at Γ, is slightly wider (0.5 eV) and crosses the Fermi level along the Γ−Z and N−X directions. The latter orbital, which has an in-plane Te(3)−Te(4) π antibonding character, is largely centered on Te(4), and therefore we shall denote it as a Te(4) lone pair. We illustrate the contributions of these types of orbitals at different points in the BZ in Figure 2a by using fat band shading (see ref 16a for more details).

To further investigate the electronic structure, we examine the DOS. In Figure 2b, we show the DOS and the partial DOS from the Te_8 rings and the Te(3), and Te(4) atoms. The partially filled flat bands lead to the presence of a sharp spike in the DOS at E_F. A quick survey of these partial DOS curves reveals that the major contributors to the orbitals at E_F are those centered on Te(4), with the next largest contribution on Te(3) and the smallest contribution from the rings. Thus, as has been seen in previous studies,[2,11,12] we too find that the atoms in the sheet are those most responsible for the electrons at the Fermi level and, hence, the conductivity properties of the solid. However, as noted above, from the charge densities for the states at E_F we find that the majority of the contribution in the DOS is associated with the 5p orbitals of the atoms in the 2D sheet that are involved in Te−Te π antibonding. To illustrate this, we show the contribution to the partial DOS of the Te(3) and Te(4) atoms for the out-of-plane π orbitals in Figure 2b. We can see from this that almost all the DOS at E_F for Te(3) is due to orbitals of this type and half of the DOS for Te(4). The remaining DOS at E_F for the latter atom is associated with the in-plane lone pair orbital as described above. This is opposed to the previously published results that find that these states are below the Fermi level and have a single Te−Te σ antibonding band partially occupied. What remains to be seen is whether there is a physical reason for this discrepancy.

To understand this bonding pattern further, we have undertaken a COHP study of the bonding within this material. The results of the COHP analysis are shown in Figure 3 for each of the Te−Te interactions present in the system. First, we note that the two symmetry-independent Te(1)−Te(2) bonds are both quite strong with an integrated COHP value of 2.30 and 2.09 eV, with essentially zero contribution at E_F. These facts are in good agreement with the assignment of the Te_8 ring as a closed-shell neutral species with single Te−Te bonds. This allows us to gauge the strengths of the other Te interactions relative to these. The Te(3)−Te(3) bonds are much smaller with an integrated COHP of almost half (1.26 eV) of those in the ring. This agrees well with the slightly increased Te−Te distance of 3.00 Å as compared to the 2.80 Å of the ring. We find a similar situation for the Te(3)−Te(4) interaction, which has an even smaller value of integrated COHP (1.06 eV) and a longer bond length (3.07 Å). As described above, only antibonding π type interactions are found below the Fermi level. Such types of interaction are undoubtedly weak as evidenced by the small band dispersion, and thus the integrated COHP of Te3−Te4 is only

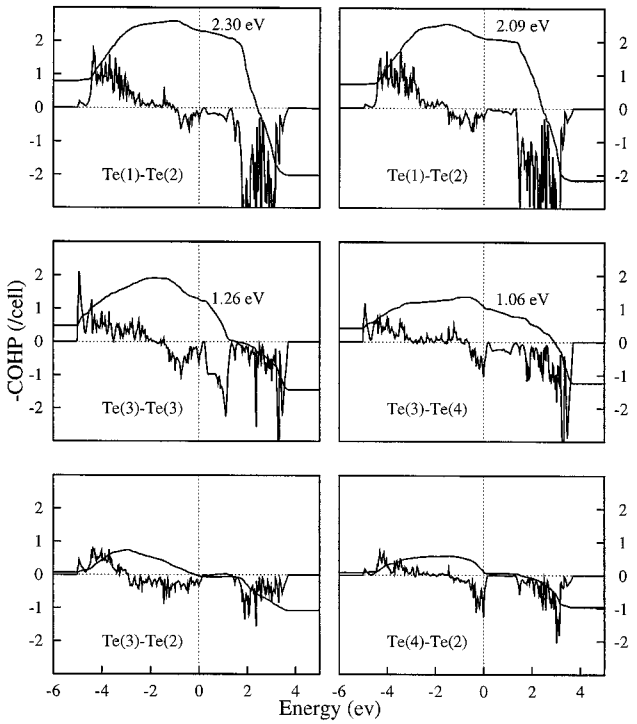

Figure 3. Crystal orbital Hamiltonian population (COHP) for the stronger Te−Te interactions in Cs_3Te_{22}. The integrated COHP value (up to the Fermi level) is given.

16% smaller than that of Te3−Te3, a value that correlates well with the small increase of the Te−Te distance.

Next we turn to the ring−sheet interactions Te(3)−Te(2) (3.41 Å) and Te(4)−Te(2) (3.44 Å). These types of interactions have integrated COHP values of essentially zero at E_F, in good agreement with the assumption that there is no direct bond between these rings and the sheet. However, we note that there is a respectable antibonding contribution just below E_F (especially for the Te(2)−Te(4) contact). These interactions are not large when compared to the direct Te−Te bonds, but the fact that they do lead to significant COHP values at lower energy suggests that the presence of the close proximity of the Te_8 rings does somewhat alter the electronic structure of the sheet by acting as an external perturbation. By inspection of the charge densities, we find that this is indeed the case. The orbitals associated with the in-plane π interactions between Te(3) and Te(4) indeed contain contributions from the orbitals on the rings, as do the out-of-plane π orbitals. We note that the authors of ref 11 have also performed a calculation that contains the Te_8 ring in the unit cell and found a similar pattern where the Te_8 orbitals interact with those of the sheet. However, they based their orbital analysis only on the calculation with the isolated sheet. Our result suggest that the close proximity of the ring to the sheet alters the electronic structure of an isolated slab[22] in a way that leads to different states at E_F. This ring−sheet interaction first changes the character of the in-plane orbital close to E_F and second pushes one out-of-plane π antibonding orbital above the E_F. Such a change in the electronic structure, as induced by the Te_8 rings, means the material may well have localization or metallic properties different from those previously reported.

Now that we have established a physical reason for the discrepancy of our results and those of the previous studies, it remains for us to provide an interpretation of the structure and bonding within the Te_6^{3-} sheet. We consider first the s orbitals that form six bands around −10 eV in our calculation. These

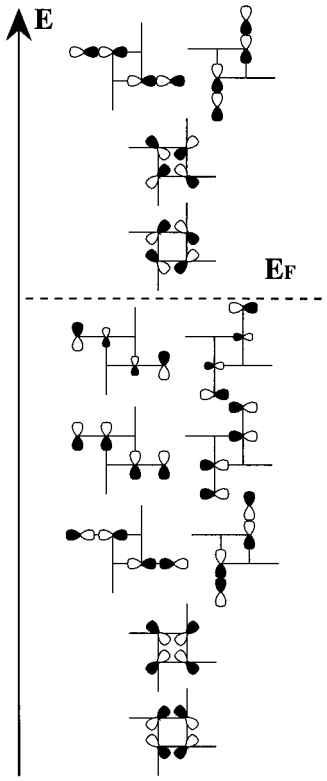

Figure 4. Schematic representation of the crystal orbitals at the special point Γ for the $CsTe_6$ layer. Only the states built from the in-plane Te 5p orbitals are represented.

orbitals account for 12 of the 39 valence electrons in the sheet. Furthermore, we find that the Te 5s do not strongly mix with the Te 5p states, which is in good agreement with the observation of bond angles of 180 and 90° in the sheet. We find also the 5p orbitals that are oriented perpendicular to the sheets are involved in six bands, one of which is partially occupied. These bands account for about 11.5 electrons. Because both series of orbitals are almost completely occupied, they do not provide much novel information about the bonding in the sheet and, therefore, need not be considered in great detail. Thus, the orbitals of the 5p in-plane interactions are much more instructive for our present purpose. We illustrate the orbitals of the slab schematically as obtained from the charge densities at the special point Γ[23] in Figure 4. The lowest in energy of these two orbitals corresponds to Te(3)−Te(3) bonding orbitals and accounts for 4 of the valence electrons. The presence of these two orbitals points to the fact that the Te(3) atoms may be described as existing in a four-member ring. The corresponding antibonding versions of these orbitals lie just above E_F. The next two orbitals (doubly degenerated at Γ) correspond to Te(3)−Te(4) bonding and account for a further 4 electrons. The antibonding versions of these orbitals form the two highest unoccupied bands. The clear separation of Te(3)−Te(4) and Te(3)−Te(4) bonding orbitals suggests that the structure of the slab consists of four-member rings interlinked by individual Te atoms. The next four orbitals (two doubly degenerated sets at Γ) correspond to both the bonding and antibonding in-plane π bond orbitals. As these sets are almost completely occupied, we may ascribe them to nonbonding lobes of the Te(3) and Te(4) sites. These four orbitals account for the remaining 7.5 electrons in the sheet. Thus, this orbital scheme suggests, in accordance with refs 2 and 12, that the best view of the 2,3-connected sheet is that of a square joined by bridging Te atoms.

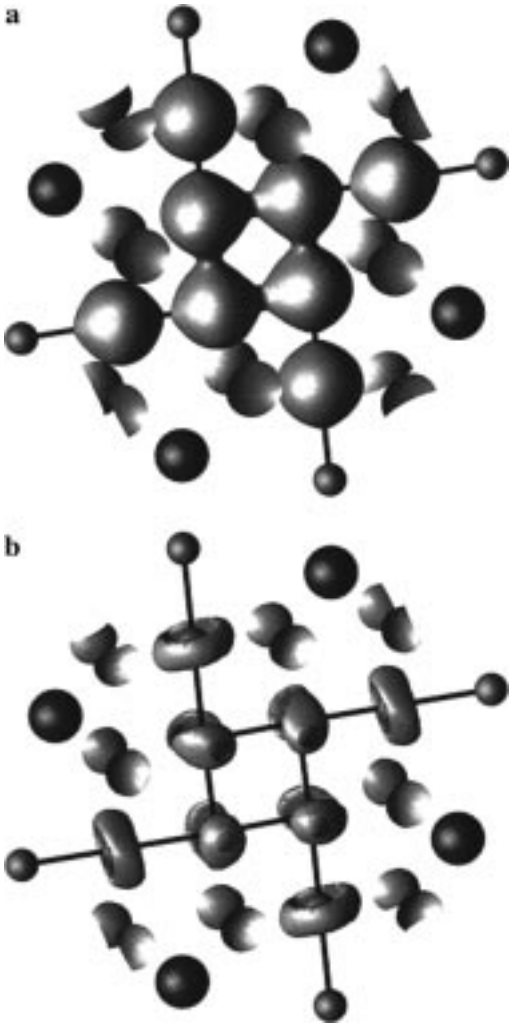

Figure 5. (a) Isosurface of 0.035 e/au^3 for the electronic density around the $CsTe_6$ layer in Cs_3Te_{22}. (b) Isosurface of 0.85 e/au^3 for the electron localization function (ELF) around the $CsTe_6$ layer in Cs_3Te_{22}.

To explore the electronic structure in terms of the density instead of orbitals, we present in Figure 5 the in-plane total charge density and the ELF. We first discuss the total charge density, where a density isosurface of 0.035 e/au^3 is presented. In this figure we see a larger electron density in the Te(3)−Te(3) bond than in the Te(3)−Te(4) bond. A maximum value of 0.0410 e/au^3 is found along the Te(3)−Te(3) bond in contrast with a maximum value of 0.0335 e/au^3 found along the Te(3)−Te(4) bond. This correlates with the above description of the sheet as being squares interconnected by Te(4) atoms and also with our observation that Te(3)−Te(3) bonds are slightly

(22) To more accurately compare our results with those of the previous studies, we have reproduced these using identical parameters and the YAeHMOP program (G. A. Landrum; freely available at http://overlap.chem.cornell.edu: 8800/yeahmop.hmtl). We have also performed the calculations within the body-centered cell and full Cs_3Te_{22} structure, including Cs atoms. We find that this combination gives a result for the band structure remarkably similar to that presented in Figure 2a. On analysis of the orbitals, we find that the two bands that we place at E_F are also at, or just below, the Fermi level in the eH calculation. The major difference is that the highest band from the eH calculation is as described in refs 2, 11, and 12 but mixes with the other two bands especially at the special point N. All three of these bands are essentially degenerate at Γ. Thus, as noted in ref 11, the eH results also indicate that there is a significant ring−sheet interaction.

(23) We illustrate these orbitals at the Γ point however, since all these bands except two are completely occupied. A more extensive examination in terms of many **k** points does not alter our arguments. We use the orbitals as they exist at Γ because the high symmetry allows a much simpler presentation.

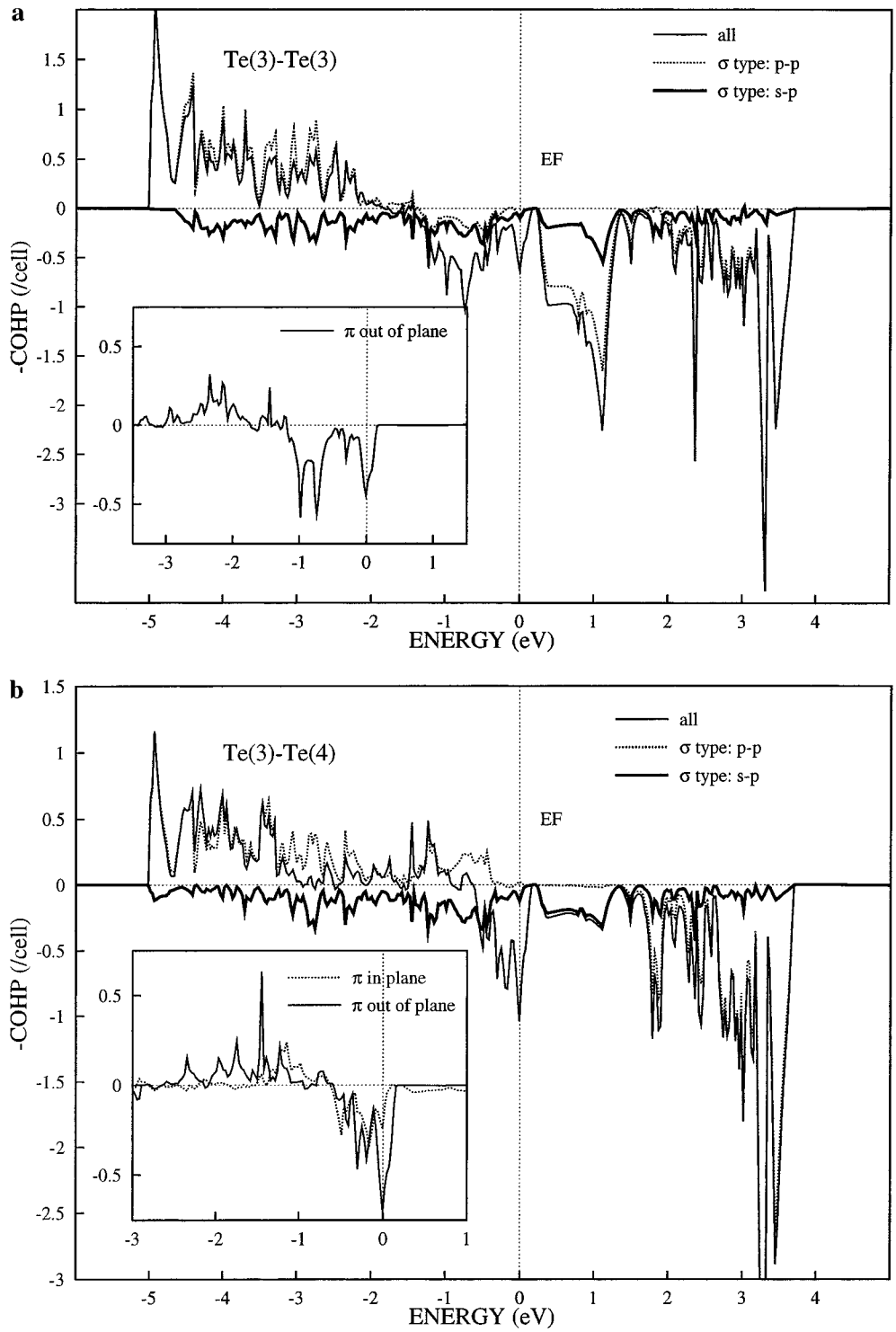

Figure 6. Detailed COHP curves for the Te(3)−Te(3) (a) and Te(3)−Te(4) (b) interactions. The curves are decomposed into orbital contributions of s−p σ, p−p σ, p−p out-of-plane π bonding, and p−p in-plane π bonding. The latter two types of interactions are shown in the inserts.

stronger then Te(3)−Te(4) bonds. We also include the charge on the Te_8 rings in this figure to show the close contact between the density of the Te(2) position and the 2,3-connected sheet.

We compare this with the ELF. The ELF function is large in regions of space where two electrons with antiparallel spins are paired and, thus, can be used to determine the degree to which electrons are localized. In a nutshell, the topology of this function allows us to understand where the electrons are localized in space and to identify features such as lone pairs, as well as to characterize the bonding within a particular material. The ELF function is normalized between zero and unity, where values closer to unity correspond to high localization. A free-electron gas has a reference value of $^1/_2$. We plot the ELF = 0.85 isosurface in Figure 5b. In this representation, regions of high electron localization (0.85 < ELF < 1) are found within the isosurface. Here the ELF reveals that the electrons are indeed strongly localized. We find a high-ELF region on the Te(4) site in the shape of a ring ($ELF_{max} = 0.89$) indicating the presence of localized nonbonding lone pairs. This is in agreement with our assignment of the in-plane π antibonding orbitals as mainly a Te(4) lone pair. The Te(3) site has two highly localized regions ($ELF_{max} = 0.94$) at each site, one above

the plane and the other below. The ELF regions on Te(3) collapse into a ring, similar to that found on Te(4), at a value of ELF = 0.79, indicating that the in-plane electron density on Te(3) is less localized than those out of the plane. The Te(3) isosurfaces combine into one single region over all four Te(3) sites at a value of ELF = 0.54 and a similar contact between Te(3) and Te(4) is found at ELF = 0.44. The latter facts correlate well with our description of the sheet containing Te_4 rings connected by single Te atoms. We also display the lone pairs on the Te(2) atoms within the ring. These lone pairs in the rings have values of ELF similar to those within the sheet. Thus, we can conclude that the electrons within the sheet and, more importantly, those within the orbitals around E_F are localized. These large-ELF regions, i.e., localized electrons, raise the question of whether this sheet is perhaps magnetic (localized) rather than metallic. We do not locate a maximum of ELF within the plane of the slab on the Te(3) site, indicating that these are not localized states, as described in ref 11. Thus, our DFT-based scheme suggests not only that the material is, most likely, an insulator, but that the magnetic state is different from that previously reported.

To examine this, we return to our COHP for the interactions within the sheet. The fact that there are only four electrons in both the Te(3)−Te(3) and Te(3)−Te(4) σ bonding orbitals strongly correlates with our calculated integrated COHP values that are approximately half that of a Te−Te single bond. If these bonds were single bonds, they would require twice this number of electrons. Figure 6 shows a decomposition of the Te(3)−Te(3) and Te(3)−Te(4) COHP curves in terms of the σ and π components of the interactions. The largest interactions at E_F are the Te−Te π antibonding orbitals. These interactions are Te(3)−Te(3) out-of-plane π (COHP(E_F) = −0.5), Te(3)−Te(4) out-of-plane π (COHP(E_F) = −0.7), and Te(3)−Te(4) in-plane π (COHP(E_F) = −0.3). The largest Te−Te σ antibonding interactions occur for both bonds above the Fermi level. Both p−p σ antibonding and s−p σ antibonding interactions are very small and have almost no contribution at E_F. This small s−p interaction is largely due to the clear separation of s from p states as obtained in our calculation, and the small p−p type is due to the fact that the strong σ antibonding orbitals are above E_F. Thus, we see that almost all the electrons at E_F are within the π network (either in or out of the plane of the sheet). Therefore, the conduction electrons are associated with these weaker π bands and have almost no σ character. As noted above the π bonding leads to flatter bands at E_F and, therefore, to regions of high ELF.

Let us now speculate on the ramifications of these results with regard to the electronic properties of this material. First, if the system is a metal, then the result of having interactions between the 2,3-connected Te_6^{3-} sheet and the Te_8 rings suggests that one will undoubtedly find a type of conductivity different from that previously reported. Indeed, we have found a different Fermi surface that contains components in all three directions. Thus, the material should be a 3D conductor. However, we were not able to find, as suggested by Canadell et al.,[2] a suitable **q** vector on our Fermi surface that could lead to complete nesting.

The large Te−Te inter-ring contact distances (3.80 Å) in the *c* direction indicate that the system will have a low conductivity in that direction. However, we find that the electronic velocities are even smaller in the remaining directions and thus the whole system may be a poor conductor. The close proximity of the ring pushes the Te−Te π^* interactions in the sheet up to E_F and leads to less dispersive partially occupied bands, which suggests the system is indeed likely to be an insulator. If the system is localized, then one must address the question, In which type of localized state is it? Our ELF results rule out the previously suggested radical lobes within the plane of the slab on the Te(3) site. The description of the slab as a combination of $Te(3)_4$ squares and Te(4) atoms points the way. If the system were indeed localized, then a likely possible description would be that the sheet is composed of $Te(4)^-$ atoms that interconnect $Te(3)_4^-$ rings. The $Te(3)_4^-$ squares would contain one unpaired electron, which resides, according to our charge analysis, in the π orbitals above and below the plane of the slab.

Conclusion

We find that the close contacts between Te_8 rings and the 2,3-connected square sheet of the compound Cs_3Te_{22} play an important role in the electronic structure of this material. On the basis of our results, we conclude the system may indeed be an insulator, but the magnetic state is different from that previously reported. A study of the magnetic and electrical properties of this material therefore is highly desirable.

Acknowledgment. F.B. thanks the Max-Planck-Gesellschaft and the CNRS for financial support. We also express our thanks to Prof. Enric Canadell for his comments on the paper.

IC9714605